Reassessment of the electron density in Cu_2O using γ-ray diffraction

W. Jauch and M. Reehuis

Helmholtz-Zentrum Berlin für Materialien und Energie, Hahn-Meitner-Platz 1,

D-14109 Berlin, Germany

Abstract

The electron density distribution in Cu_2O has been critically reexamined to test controversial conclusions from earlier experimental and theoretical studies. The electron density is derived *via* multipole refinement of high-quality single-crystal diffraction data, collected at room temperature with 316.5 keV gamma radiation. Four γ-lines in the energy range 200 – 600 keV have been used to extrapolate extinction-free low-order structure factors. The remaining extinction corrections refine to a crystal mosaicity identical to the observed one. There is no support for anharmonic contributions to the thermal parameters. Important features of the derived electron density are (i) a partially filled d_z^2 orbital, (ii) an incomplete ionization of Cu and O, (iii) no interstitial Cu–Cu charge pileup, thereby refuting the covalent bonding hypothesis.

I. Introduction

Cuprite (Cu_2O) has attracted considerable interest because it is a parent compound of the copper oxide high-temperature superconductors. It was used as a benchmark system in several feasibility studies to test the effect of different radiation sources on the quality of the derived electron density. Employed experimental techniques comprise laboratory Ag $K\alpha$ (Restori and Schwarzenbach, 1986) and synchrotron radiation of both 0.56 Å (Kirfel and Eichhorn, 1990). Synchrotron radiation of even higher energy, 100 keV (0.12 Å), was applied by Lippmann and Schneider (2000*a,b*, LSa and LSb hereafter). Zuo *et al.* (1999) used convergent-beam electron diffraction to measure low-order reflections which were merged with higher-order structure factors taken from reported x-ray measurements. There are substantial discrepancies between the different studies. LSa,b do not confirm Cu – Cu covalent bonding, inferred from an interstitial non-nuclear maximum, as well as the effective charge transfer from Cu to O, reported by Zuo et al. (1999). Zuo (2004) argues that the discrepancies are due to systematic errors in the first four reflections {110, 111, 200, 211}, and asks for a careful reexamination of the *x*-ray data.

It is the purpose of our study to meet these objections and to clarify the mutual discrepancies. In order to improve the reliability of results γ-rays from ^{192}Ir at 200 – 600 keV are chosen as radiation source. Besides improvement in accuracy due to the probing energy, an inherently stable beam of narrow spectral band width is provided. A further benefit is the capability to measure intensity data to high order. A detailed analysis of the charge distribution in Cu_2O will be presented.

II. Data collection and reduction

The single crystal of Cu_2O was purchased from MaTecK/Jülich. Cuprite crystallizes in the cubic space group $Pn\bar{3}m$ with Cu at site 4*b* (0,0,0) and O at site 2*a* (¼,¼,¼) which have point

symmetry $\bar{3}m$ and $\bar{4}3m$, respectively. Fig. 1 shows that each Cu atom is linearly coordinated by two oxygen atoms, and all oxygen atoms are tetrahedrally surrounded by four Cu atoms.

From high-resolution γ-ray rocking curves, using a perfect Si-crystal as a collimator (angular resolution: 1.5" of arc), the intrinsic mosaic width can be obtained in a direct manner. Rocking curves were taken along three perpendicular directions. The diffraction profiles were isotropic with Gaussian full widths at half maximum (FWHM) of 10.0(3), 10.0(3) and 10.5(3)" of arc, so that secondary extinction is expected to be pronounced. The low-order reflections were therefore determined at three additional γ-energies, thereby allowing the access to extinction-free values.

The diffraction data have been collected on the four-circle gamma-ray diffractometer at the Helmholtz-Zentrum Berlin. Reflection intensities were measured in ω-step scan mode with an intrinsic germanium detector. The counting time for each reflection was individually adjusted to ensure similar statistical precision in the intensities. An absorption correction was performed by the analytical method implemented in the *Xtal* suite of crystallographic programs (Hall et al., 1995). Crystal data and experimental conditions are summarized in Table 1.

Reflections with Miller indices of parity *eeo* (*e* = even, *o* = odd) had intensities too small to be measured with γ–rays. As shown by Kirfel & Eichhorn (1990), they are dominated by U_{12}(Cu), containing very little information about electronic deformation. In order to fix the anisotropy of the copper atomic vibrations, 18 of these very weak reflections were taken from LSa.

Coherent one-phonon scattering from acoustic modes of vibration is the dominant contribution to thermal diffuse scattering (TDS) and has been calculated using the formalism of Skelton & Katz (1969). For the experimental conditions that apply to this work (small Bragg angles, ω-scan, circular detector window), the expression for the TDS/Bragg scattering

ratio, α, reduces to a very simple formula with a $(\sin\theta/\lambda)^3$ dependence. With elastic constants from Hallberg & Hanson (1970), the maximum correction term was $\alpha = 0.092$.

III. Extrapolation to zero wavelength

The wavelength dependence of extinction can be well described by suitable theoretical models (Palmer and Jauch, 1995, Jauch and Palmer, 2003). According to Zachariasen (1967), the extinction coefficient, defined by $y = I_{obs}/I_{kin}$ as the ratio of the observed integrated intensity to its kinematical value, has the simple form $y = (1 + 2x)^{-1/2}$ with $x = g\overline{T_\mu}\,\lambda^2(F/V)^2 d$ for high-energy diffraction from a mosaic crystal with a Gaussian tilt angle distribution (g = 0.6643/FWHM [rad], $\overline{T_\mu}$ = absorption-weighted mean path length of diffracted beam, F = kinematical structure factor in units of scattering length, V = unit cell volume, d = interplanar distance).

Four γ-lines of wavelength 0.0205, 0.0265, 0.0392 and 0.0602 Å were used to determine the five strongest kinematical structure factors. For inter-wavelength scaling (incoming flux, detector efficiency), a few reflections of intermediate intensity have been measured to 1% counting statistical precision or better. Their absolute values are known from the accurate standard structural parameters, with remaining weak extinction being taken into account.

The wavelength-dependent data were fitted to Zachariasen's expression. The measurement uncertainties are composed of the counting statistical contribution and the uncertainty in the scale factors. Two parameters have been varied, the kinematical structure-factor amplitude $F(\lambda = 0)$ and the mosaic width parameter g.

IV. Data modeling

The electron density was represented as a multipole expansion of nucleus-centered functions according to the rigid pseudoatom formalism of Stewart (1976). The model charge density of Cu is decomposed into the core and the diffuse 4*s* electron, as well as the spherical and aspherical part of the 3*d* valence shell which include the symmetry-allowed real spherical surface harmonics y_{00}, y_{20}, y_{40} and y_{43+}. For O, the valence density is constructed from the average of the 2*s* and 2*p* orbitals; the higher multipole functions are y_{32-} and the Kubic harmonic K_4 (a linear combination of y_{40} and y_{44+}). The spherical harmonics are expressed relative to a global coordinate system with *z* along the threefold axis [111] and *y* along $[\bar{1}10]$.

A radial scaling parameter κ allows for joint expansion ($\kappa < 1$) or contraction ($\kappa > 1$) of the valence monopole and the higher poles (Coppens *et al.*, 1979). The radial distribution functions of neutral Cu ($^2S_{1/2}$) and O were calculated from Hartree-Fock (HF) atomic wave functions in the basis of Clementi & Roetti (1974). For Cu, the square of the radial part of the 3*d* canonical HF orbitals (5 Slater functions) was used to construct both monopole and multipoles. Radial terms for the higher poles of O were taken in the single exponential form $r^n\exp(-\alpha r)$ with $n = 3$ and 4 for octupole and hexadecapole, and a fixed standard exponent $\alpha = 4.50$ bohr^{-1}.

The *VALRAY* program (Stewart *et al.*, 2000) was used for data modeling, minimizing $\chi^2 = \Sigma w(|F_{obs}|^2 - k^2 y|F_{cal}|^2)^2$, with $w = 1/\sigma^2(|F_{obs}|^2)$ determined from Poisson statistics, F_{obs} being the observed structure factors. Two further adjustable parameters include a scale factor, *k*, and a mosaic width parameter on which the extinction factors, *y*, depend. Symmetrically equivalent reflections were treated separately to allow for differences in absorption-weighted mean path lengths.

The scale factor was determined from high-order independent-atom-model (IAM) refinements, and was fixed in later refinements with improved scattering models.

In Table 2, the quality of fit is given for the various scattering models. A large improvement of fit is already obtained on the introduction of charge transfer and valence shell expansion/contraction. The high precision of the data is reflected by the large value of χ^2 for the IAM.

The final refinement results for the multipole model are listed in Table 3. The normalization condition for the aspherical density functions is such that the coefficients correspond to the local electrostatic moments in angstrom units.

The results were obtained by using the extrapolated zero wavelength data for the 111, 200, 220, 311 and 400 reflections. It is satisfying that for {111} both extinction-free $F(\lambda = 0)$ and extinction-affected values $F(\lambda = 0.0392)$ could be used concomitantly, yielding equally acceptable residuals. It thus appears that the objective of an adequate extinction correction has been realized.

Zachariasen's extinction model was applied in the final refinements. The fitted Gaussian mosaic FWHM is 9.92(2)" of arc, which compares extremely well with the observed values. In consequence, the extinction parameter represents a physically realistic description and not a dubious fudge factor. The maximum reduction in $|F_{obs}|^2$ was 8.0%.

V. Discussion of results

A. Data quality

The ten lowest-order structure factors are listed in Table 4. The random errors of the extrapolated values are dominated by uncertainties in the scale factors, so that their precision is limited to 0.5%. The important structure factors, 110 and 111, have now been determined with a precision of 0.1% and 0.04%, respectively. Room temperature structure factors from electron diffraction are lacking so that a direct comparison with Table 4 is not possible. A comparison with theoretical values presented by Zuo (2004), however, is included in Table 4. There is good agreement between measurements and model structure factors. A most

intriguing feature is the alternation of discrepancies between experimental and theoretical results. There is acceptable accordance for the strong reflections. This is not the case for the (*ooe*) structure factors which are dominated by the oxygen monopole contribution. It seems that theory is lagging behind experiment in this case.

B. Thermal motion

Anisotropic thermal displacement of Cu can occur parallel and perpendicular to [111]. From Table 3 follows $U_{\parallel}$ = 0.01685(4) Å^2 and $U_{\perp}$ = 0.01916(3) Å^2. Thermal motion is thus larger perpendicular than parallel to the Cu – O bond, in agreement with expectation and previous x-ray results. The thermal displacement parameters reported by LSa,b for Cu and O are about 5% larger than the present values which may partly be due to different experimental temperatures.

To test the effect of anharmonicity in the thermal motion fourth-order Gram-Charlier coefficients were introduced for Cu. Combined refinement of multipole and anharmonic parameters leads to insignificant fourth-order coefficients. There is thus no support for a noticeable anharmonic component in the effective atomic potential, contrary to the conclusion of Zuo et al. (1999).

C. Valence shell parameters

The 3*d* shell exhibits a spatial contraction of 2.1(2)%. The refined charge transfer from Cu to O amounts to 0.402(14) electrons. The high precision of the parameter value (29σ) is noteworthy. It thus leads to a formal notation of $Cu_2^{+0.4}O^{-0.8}$. The charge on Cu reported by LSa,b is 0.57(3) and Kirfel et al. give 0.61(9) electrons. From quantum chemical calculations Wang and Schwarz (2000) deduce partial charges of $Cu^{+(0.5\pm0.1)}$ and $O^{-(1.0\pm0.2)}$. There is thus consistency of results. Zuo et al. (1999) find a refined charge transfer of 1.01(5) electrons, that

is, nominal ionic charges, Cu^{+} and O^{-2}. There is thus important discrepancy on this crucial point between electron diffraction and the corresponding collection of other results.

D. Asphericity of charge distribution

Following Holladay et al. (1983), *d*-orbital occupancies may be calculated from multipole population parameters. In the case of point symmetry $\bar{3}m$, the atomic *d* orbitals split into two doublets e_g, e'_g and a singlet a_g. With the *z* axis along the [111] direction, the singlet corresponds to d_z^2, $a_g(z^2)$, whereas the doublets $e_g(xz, yz)$, $e'_g(xy, x^2 - y^2)$ are composed of d_{xz}, d_{yz} and d_{xy}, $d_{x^2-y^2}$, respectively. A detailed discussion of the *d*-orbital analysis for trigonal symmetry is given by Jauch and Reehuis (2003) including a corrected orbital-multipole matrix.

The occupancies of the 9.6 electrons in the 3*d*-shell determined from the refined multipole populations are $P(a_g) = 1.77(1)$, $P(e'_g) = 3.70(3)$ and $P(e_g) = 4.13(3)$ electrons. The cross term is $P(e_g,e'_g) = 0.20(3)$. There is thus a deficit of 3*d* population along the O–Cu–O *z* axis and in the *xy* plane. There is good agreement with Zuo *et al.* (1999) who find 0.22 electrons removed from the a_g state which they estimated from a partial Cu on-site 3*d*–4*s* hybridization. The depletion of the a_g lobes is clearly reflected in the deformation map (Fig. 3). The e_g orbital has a population larger than four, so that the constraint imposed by the exclusion principle is violated. The unphysical value can be explained by overlap of the Cu and O atomic orbitals since equating the multipolar density with the *d*-orbital description is based on the assumption of negligible overlap.

Instead of y_{40} and y_{43+}, LSa,b used the Kubic harmonic K_4 as hexadecapole term on Cu which is incompatible with the actual low site symmetry. This incorrect assignment is most probably the source of the disagreement with the theoretical hexadecapole pointed out by Laskowski et al. (2003). A negative sign of P_{40} was already predicted by Restori and Schwarzenbach (1986).

Deformation density features of O are of the order of 3σ and thus at the limit of significance. According to Zuo et al. (1999), the deformation parameters of O are highly significant up to 33σ, a result which looks impossible, in particular in comparison to the Cu populations which are significant only up to 6σ.

E. Critical points

Interatomic interactions can be characterized by the values of the density $\rho(\mathbf{r}_c)$ and its Laplacian $\nabla^2\rho(\mathbf{r}_c)$ at the bond critical saddle points ($\mathbf{r}_c$) between two nuclei (Bader, 1990). Bond critical point (bcp) properties derived from the experimental model electron density are summarized in Table 5.

Two different bcp's are found. Bcp_1 corresponds to the bond between Cu and O which indicates dominant ionic interaction ($\rho(\mathbf{r}_c)$ low and $\nabla^2\rho(\mathbf{r}_c) > 0$). Bcp_2 is at the midpoint between two Cu atoms belonging to a Cu_4 tetrahedron. Both the density and the Laplacian are smaller by an order-of-magnitude than at bcp_1, and thus the nature of bcp_2 is somewhat uncertain. Bcp_2 is, however, also present in the theoretical calculation. The values found to be close to zero indicate a homogeneous distribution of electrons. Weakly metallic cation-cation bonding has indeed been suggested by Filipetti and Fiorentini (2005). The bcp properties are in agreement with previous experimental and theoretical investigations (LSb, Laskowsky et al., 2003).

Zuo et al. (1999) found a density maximum of 0.2 $e\text{Å}^{-3}$ at the center of the unoccupied tetrahedral interstitial region of the four neighboring Cu atoms which was interpreted as a direct Cu – Cu covalent bonding. In disagreement with Zuo et al. (1999), no evidence of any electron localization is found at the interstices where the charge density has absolute minima, confirming the finding of LSb. The existence of these minima is also supported by theoretical results from Filippetti and Fiorentini (2005).

VI. Concluding remarks

An extended set of high-quality structure factors, achieved by the use of 316.5 keV γ-radiation, has provided the basis for a new examination of the electron density distribution in Cu_2O. Extinction-free estimates of structure factor values have been established by energy-dependent measurements between 200 and 600 keV. This has lead to a resolution of the controversial debates surrounding the charge distribution of Cu_2O. The present results are largely at variance with the conclusions drawn from electron diffraction, whereas the correctness of previous synchrotron measurements is confirmed.

References

Bader, R. F. W. (1990). *Atoms in Molecules: A Quantum Theory*, Oxford: Clarendon.

Clementi, E. & Roetti, C. (1974). *At. Data Nucl. Data Tables*, **14**, 177-478.

Coppens, P., Guru Row, T. N., Leung, P., Stevens, E. D., Becker, P. J. and Y. W. Yang, Y., (1979). *Acta Cryst.* A**35**, 63-72.

Filippetti, A. & Fiorentino, V. (2005). *Phys. Rev. B 72*, 035128.

Hallberg, J. & Hanson, R. C. (1970). *Phys. Status Solidi* **42**, 305-310.

Hall, S. R., King, G. & Stewart, J. (1995) Eds. *Xtal3.4 User's Manual*. University of Western Australia: *Lamb, Perth*.

Holladay, A., Leung, P. & Coppens, P. (1983). *Acta Cryst.* A**39**, 377-387.

Hubbell, J. H. & Seltzer, M. S. (1995). National Institute of Standards and Technology Internal Report 5632; also available via http://www.physics.nist.gov/PhysRefData/XrayMassCoef/cover.html.

Jauch, W. & Palmer, A. (2002). *Acta Cryst.* A**58**, 448.

Jauch, W. & Reehuis, M. (2003*). Phys. Rev. B* **67**, 184420.

Kirfel, A. & Eichhorn, K. (1990). *Acta Cryst.* A**46**, 271-284.

Laskowsky, R., Blaha, P. & Schwarz, K. (2003). *Phys. Rev. B* **67**, 075102.

Lippmann, T. & Schneider, J. R. (2000*a*). *J. Appl. Cryst.* **33**, 156-167.

Lippmann, T. & Schneider, J. R. (2000*b*). *Acta Cryst.* A**56**, 575-584.

Palmer, A. & Jauch, W. (1995). Acta Cryst. A**51**, 662-667.

Restori, R. & Schwarzenbach, D. (1986). *Acta Cryst.* B**42**, 201-208.

Skelton, E. F. & Katz, J. L. (1969). *Acta Cryst.* A**25**, 319-329.

Stewart, R. F. (1976). *Acta Cryst.* A**32**, 565-574.

Stewart, R. F., Spackman, M. A. & Flensburg, C. (2000). *VALRAY User's Manual*. Carnegie Mellon University, USA, and University of Copenhagen, Denmark.

Wang S.-G. & Schwarz, W. H. E. (2000). *Angew. Chem. Int. Ed.* **39**, 1757-1762.

Wyckoff, R. W. G. (1963). *Crystal Structures Vol. 1*, 2nd ed., New York: Interscience.

Zachariasen, W. H. (1967). *Acta Cryst.* **23**, 558-564.

Zuo, J. M., Kim, M., O'Keefe, M. & Spence, J. C. H. (1999). *Nature* **401**, 49-52.

Zuo, J. M. (2004). *Rep. Prog. Phys.* **67**, 2053-2103.

Table 1

Experimental details. The linear absorption coefficient μ is obtained from Hubbell & Seltzer (1995). $\overline{T_\mu}$ denotes the absorption-weighted mean path length through the crystal. The lattice constant is taken from Wyckoff (1963).

Temperature (K)	295 (ambient)
Lattice constant (Å)	4.2696
Crystal size (mm)	2.25×2.38×2.64
Wavelength (Å) / Energy (keV)	0.0392 / 316.5
Scan width (°)	0.7
Steps/scan	111
μ (cm^{-1})	0.6564
Transmission range	0.862 – 0.875
$\overline{T_\mu}$ range (mm)	2.02 – 2.25
Reflections used	200
Unique reflections	82
$(\sin\theta/\lambda)_{max}$ ($Å^{-1}$)	1.28
Overall counting-statistical $\Sigma\sigma(I)/\Sigma I$	0.0083

Table 2

Quality of fit for the various scattering models. *Np* = number of adjustable parameters. In all cases, the scale factor was fixed to the value obtained from high-order IAM refinements.

	IAM	Monopoles	Multipoles
χ^2	8116.8	826.6	481.6
Np	4	7	12

Table 3

Multipole refinement results. Reliability factors: $R(F) = \sum|F_{obs} - F_{cal}|/ \sum|F_{obs}|$, $wR(F^2) = [\sum w(F_{obs}^2 - F_{cal}^2)^2 / \sum wF_{obs}^4]^{1/2}$, reduced chi-square $\chi_r^2 = \chi^2 /$ (degrees of freedom).

Cu	U_{11} (Å^2)	0.01839(2)
	U_{12} (Å^2)	–0.00077(2)
	$\kappa_0 = \kappa_2 = \kappa_4$	1.021(2)
	P_{00} (|e|)	9.598(14)
	P_{20} (|e|Å^2)	–0.483(32)
	P_{40} (|e|Å^4)	–0.069(29)
	P_{43+} (|e|Å^4)	–0.458(97)
O	U (Å^2)	0.01781(13)
	κ	1.006(6)
	P_{00} (|e|)	6.805(28)
	P_{32-} (|e|Å^3)	–0.297(98)
	P_4 (|e|Å^4)	–0.204(74)
$R(F)$, $wR(F^2)$		0.0078, 0.0099
χ_r^2		2.503

Table 4

Extinction-corrected experimental and calculated low-order structure factors (electrons per unit cell) of Cu_2O at room temperature. The theoretical structure factors are taken from Zuo (2004); they are calculated by the linearized augmented plane wave method (LAPW) using the local density approximation (LAPW RT). $R(F) = \sum|F_{obs} - F_{cal}| / \sum|F_{obs}| = 0.0073$, $R(\sigma) = \sum\sigma(F_{obs}) / \sum|F_{obs}| = 0.0036$.

hkl	$\sin\theta/\lambda$ (Å^{-1})	F_{obs} (γ-ray)	F_{cal} (multipole)	F_{cal} / F_{theory}
110	0.166	12.813(13)	12.812	1.067
111	0.203	87.566(33)	87.560	1.006
200	0.234	71.95(36)	71.543	1.003
211	0.287	8.385(31)	8.430	1.063
220	0.331	71.49(36)	70.594	1.019
310	0.370	6.158(32)	6.150	1.078
311	0.388	54.65(27)	54.095	1.013
222	0.406	45.940(75)	46.254	1.002
321	0.438	3.852(73)	4.028	1.067
400	0.468	46.59(23)	46.017	1.017

Table 5

Properties of the bond critical points and the (3,+3) minimum. Values of $\rho(\mathbf{r})$ in eÅ^{-3}, values of $\nabla^2\rho(\mathbf{r})$ in eÅ^{-5}.

		r	$\rho(\mathbf{r})$	$\nabla^2\rho(\mathbf{r})$
bcp_1 (Cu – O)	Expt.[a]	0.1228 , 0.1228 , 0.1228	0.830	14.877
	Expt.[b]	0.1227 , 0.1227 , 0.1227	0.816	14.872
	Theory[c]	0.1231 , 0.1231 , 0.1231	0.794	13.0
bcp_2 (Cu – Cu)	Expt.[a]	0.75 , 0.25 , 0	0.087	0.562
	Expt.[b]	0.75 , 0.25 , 0	0.092	0.607
	Theory[c]	0.75 , 0.25 , 0	0.116	0.47
local minimum	Expt.[a]	0.75 , 0.25 , 0.25	0.065	0.288
	Expt.[b]	0.75 , 0.25 , 0.25	0.068	0.325
	Theory[c]	0.75 , 0.25 , 0.25	0.077	0.51

[a] present work [b] LSb [c] Laskowsky *et al.* (2003)

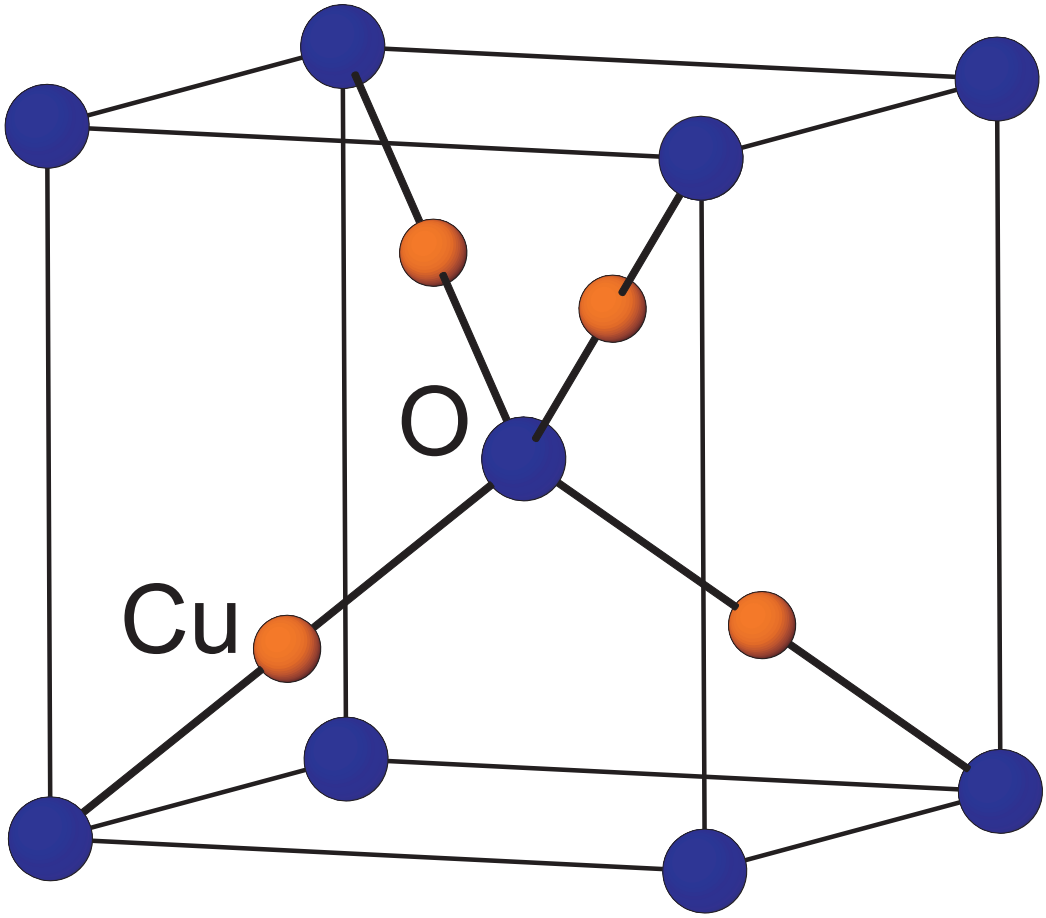

FIG. 1. Crystal structure of Cu_2O. To simplify the structure plot we used origin choice 1 of space group $Pn\bar{3}m$ with Cu at site 4*b* (¼,¼,¼) and O at site 2*a* (0,0,0), respecticely.

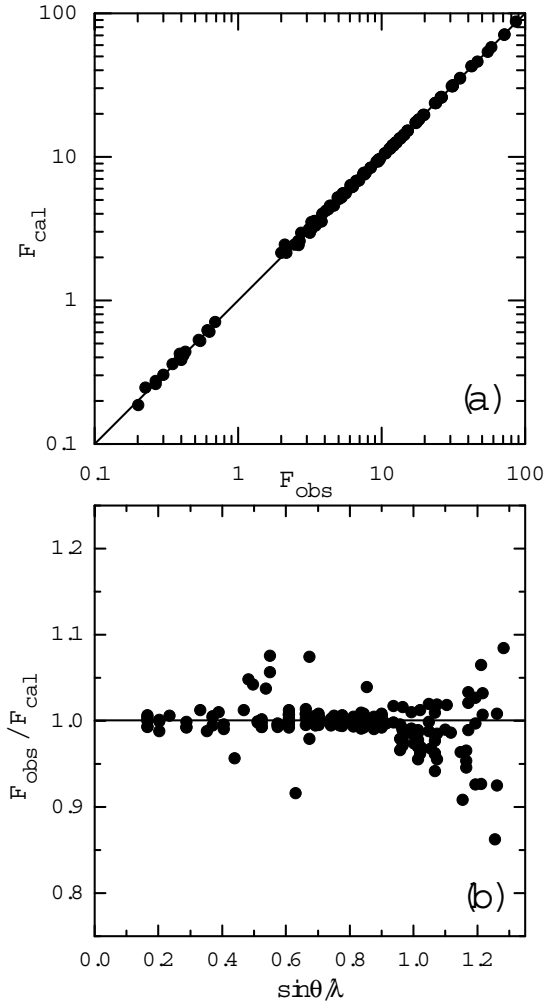

FIG. 2. (a) Scatter plot depicting the variation of variation $F_{obs}$and F_{cal}. Observed structure factors smaller than 1 were taken from LSa. (b) Variation of F_{obs}/F_{cal} with (sinθ/λ).

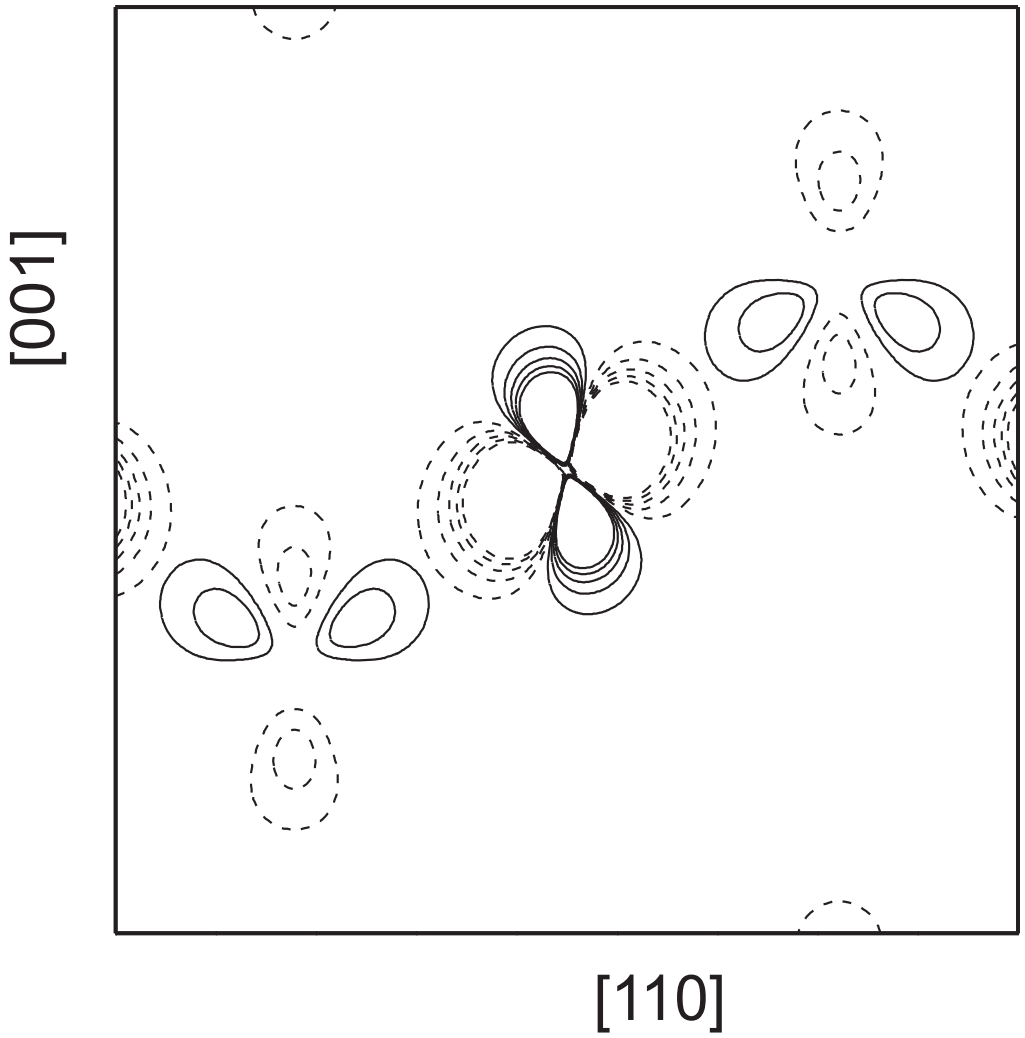

FIG. 3. Aspherical contributions to the static model density in the (110) plane with copper at the center. The density range is from –3.15 to 1.67 eÅ^{-3}. Solid lines represent regions of excessive density, dashed lines depleted regions in steps of 0.04 eÅ^{-3}. The zero contour is omitted. The densities are truncated at ± 0.2 eÅ^{-3}.